

SALVAGE: A Novel System for Interference Mitigation in FMCW RADARs

SHUBHAM JAIN, University of California, San Diego, USA

With advances in vehicular technology such as ADAS and safety features, RADARs have become an essential part of any automobile today. As such technologies become more pervasive, RADARs operating at mmWave frequencies are frequently the sensor of choice owing to their robustness, cost, range, and size. Increasing market penetration however also increases their exposure to interference from other vehicles equipped with similar RADARs [1]. Many studies carried out to understand the impact of co-vehicular interference on performance report substantial degradation in SINR under interference conditions. This paper proposes a mitigation strategy which allows us to recover data from an interfered frame with minimal processing overhead. This is done by detecting interference early in the processing chain and isolating the healthiest chirp in a frame to extract position information. This technique is tested in simulation and an improvement of up to 30% in the true positive rates is observed.

Additional Key Words and Phrases: FMCW, RADARs, Interference, FFT, NDMC

ACM Reference Format:

Shubham Jain. 2018. SALVAGE: A Novel System for Interference Mitigation in FMCW RADARs. *ACM Trans. Graph.* 37, 4, Article 111 (August 2018), 6 pages. <https://doi.org/XXXXXXX.XXXXXXX>

1 INTRODUCTION

A typical on road scenario has vehicles many of which are equipped with a variety of RADARs. These include those used for Collision avoidance, Lane Change Assist, Blind Spot detection etc.

Any RADAR is said to have been Interfered with when the transmitted pulses from any of the other RADARs combine with target reflections and corrupt its signal. The nature and mechanisms of these interactions have been covered in detail in [2] and [3]. Broadly, there exist two scenarios of interference between two FMCW RADARs based on their sweep slopes (k). Hereon referred to as the Ego (victim) and Interferer (Aggressor):

- $k_{ego} = k_{int}$: This scenario results in a ghost peak appearing in the RangeFFT results of the victim radar.
- $k_{ego} \neq k_{int}$: This scenario results in the energy (contained in IF band of victim RADAR) from the interfering signal being distributed uniformly across RangeFFT bins causing an increase in the noise floor.

In a typical scenario, we don't expect vehicles on road to have the same slope as they are dependent on the manufacturer and chosen based on speed, resolution requirements etc. This makes the second case above much more probable. Further, owing to the $1/d^2$

Author's address: Shubham Jain, s2jain@ucsd.edu, University of California, San Diego, 9500 Gilman Drive, La Jolla, California, USA, 92092.

Permission to make digital or hard copies of all or part of this work for personal or classroom use is granted without fee provided that copies are not made or distributed for profit or commercial advantage and that copies bear this notice and the full citation on the first page. Copyrights for components of this work owned by others than ACM must be honored. Abstracting with credit is permitted. To copy otherwise, or republish, to post on servers or to redistribute to lists, requires prior specific permission and/or a fee. Request permissions from permissions@acm.org.

© 2018 Association for Computing Machinery.

0730-0301/2018/8-ART111 \$15.00

<https://doi.org/XXXXXXX.XXXXXXX>

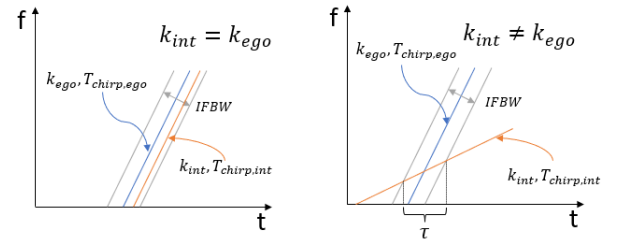


Fig. 1. The mechanisms of interference in FMCW RADARs

attenuation faced by an interfering pulse; as compared to the $1/d^4$ attenuation that a target reflection goes through, interference signals tend to be much stronger and can drown out target reflections or even saturate the receiver. In [4], Authors found that these can lead to FIT rates exceeding the ASIL C and D level requirements. Thus, rendering the RADAR unusable for critical systems. In [5], authors simulated various on road scenarios and found that interference from head on RADARs can severely impair the tracking system. In the worst case, they observed a reduction of 89% in the distance from which a terminal track could be plotted by said system. This worst-case scenario of different k , head on interferer is what has been considered for evaluation in this paper.

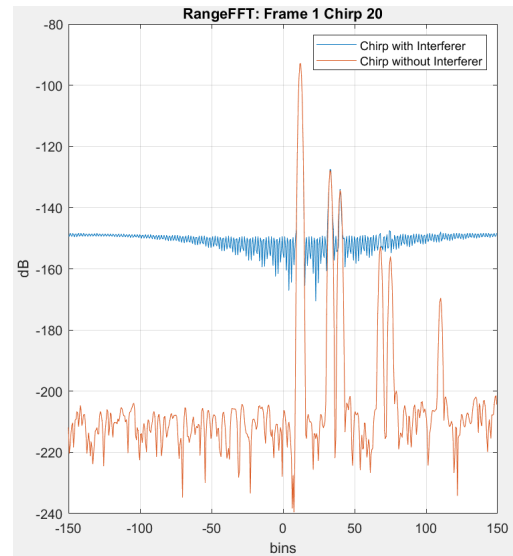


Fig. 2. RangeFFT showing increase in noise floor due interferer with different slope

An ideal solution to this problem should have the ability to extract range, angle and velocity information from a frame interfered with by multiple interferers. Further, since these are independent and critical systems, it should try to minimize:

- Processing Overhead.
- Dependence on cooperation from other RADARs
- Hardware Modifications needed for implementation

Section 2 contains a detailed discussion of related works. It is important to note that most of the proposed solutions for Interference Mitigation in literature fail on one or multiple of the above requirements.

Section 3 will introduce the proposed algorithm. It is based on the insights that Interference and Reflections appear distinct in the RangeFFT of a complex baseband receiver. And that not all bins on all chirps in a frame are affected equally by an interferer. The proposed system was found to improve True Positive Rates by up to 30% in simulations for the worst-case scenario described above.

A detailed look at the simulator implementation and evaluation of results is presented in Sections 4 and 5.

2 BACKGROUND AND RELATED WORK

Prior work in this field has been covered in extensive detail in [4] and some prominent techniques have been highlighted here. Broadly, this study divides up literature into three categories

2.1 Hardware/Architecture Based Schemes

These techniques call for a fundamental change in hardware architecture such as the Antenna or Transceiver. In [6], authors use opposing circular polarizations on transmit and receive antennas to increase Polarization Loss for interferers. However, the large antenna size and potentially reduced effectiveness in rainy weather make this scheme unattractive. In [7], authors have used a matched filter on a PMCW RADAR to successfully remove interference. But this is not applicable to the FMCW-FMCW interference scenario we are considering.

2.2 Avoidance Techniques

These techniques either the transmitted pulse in time or frequency domain to move the interferer's pulse out of the victim RADAR's IF BW. This was analysed in [8] but only for the same k case. Experiments conducted for the different k case conclude that it isn't effective by itself in giving any significant interference reduction. Especially as the number of interferers rises. This can also be seen from the results in Section 5.

Dithering in frequency on the other hand requires allocation of mutually exclusive frequency bands which is limited by the available BW. Strategic approaches such as the one in [9] rely on a functional V2X communication channel to negotiate resources. While this class of solutions is the most organized and robust method of avoiding interference, the prerequisite of a communication channel make them impractical.

2.3 Mitigation Techniques

These techniques attempt to extract information out of an interfered chirp. Further, they can be divided into:

- Time domain Techniques: A common approach is to excise the corrupted samples in time domain before processing. In [10], authors find the samples to excise based on a novel thresholding method. Replacing these directly with zeros

leads to noise in frequency, and so authors in [11] use RRC windows to obtain better spectral performance.

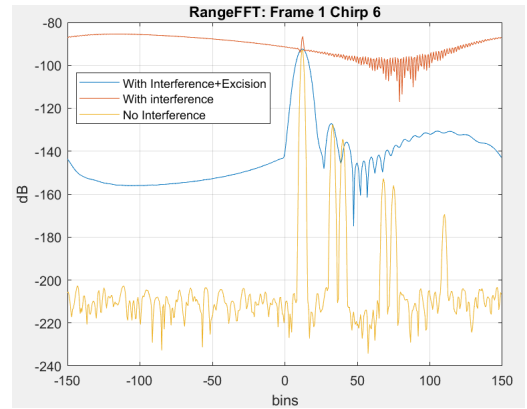


Fig. 3. Time Domain excision show improvement in SNR

While these methods show a clear improvement in the Signal to Interference and Noise Ratio (SINR), they work well only when the number of affected samples is small in comparison to chirp length. As affected samples grow with interferers, too much information is lost in the excision and we lose out on resolution.

An alternative solution is presented in [12] where the authors try to estimate the Amplitude, frequency, and phase of the interfering pulse. And then use this information to cancel it out in time domain. However, this approach is computationally intensive, and the maths presented is applicable for a single interferer only.

- Time and Frequency Domain: An innovative approach has been outlined in [14] where the authors use the MSER algorithm on a spectrogram image. Based on the results, they isolate a slow ramping interferer chirp and precisely ignore the affected samples per chirp. However, in the case under consideration for this paper, we expect the ramps to be varied and intersecting. And as it becomes more difficult to isolate them as one continuous region, the MSER algorithm's performance will degrade. No evidence has been provided in [14] to prove efficacy with multiple intersecting interferers.
- Frequency Domain Techniques: In [13], authors use the fact that interference artefacts appear on both sides of DC in the RangeFFT to try and cancel its effect using LMS filtering. This approach was replicated but no appreciable improvement in SINR could be seen.

Non-Mutual Data Cancellation, an approach used in [15] exploits the fact that interference will only increase the per bin magnitude of RangeFFT. It uses a min operator on every range bin across chirps to find the best possible RangeFFT from a given frame. A shortcoming of this approach is that it only concerns itself with magnitude of RangeFFT and ignores the phase. Thereby losing out on Angle and Velocity information.

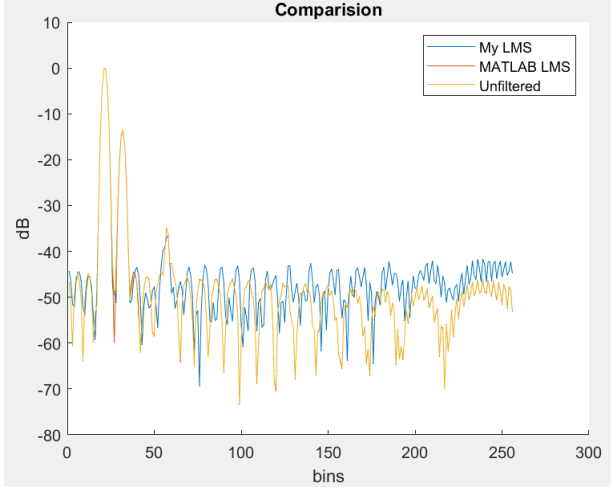


Fig. 4. LMS filter was unable to get improvements in SNR mentioned in [13]

3 DESIGN

This method proposed in this paper attempts to treat and solve this problem at a system level. There are three key insights which are used here:

- (1) Complex Baseband Receiver: As outlined in [16], when using a complex baseband receiver, all target reflections will appear in the positive half of the frequency spectrum. Whereas the noise spread due to interference will be uniform in both negative and positive bins, ideally as complex conjugate of each other. This is based on the fact that while all target reflections appear with some delay at the receiver and only appear in the positive half of the IF filter, a different k interferer's chirp will move across the IF BW and appear in both. Thus, we can use the power in negative half of RangeFFT to tag a chirp as clean or noisy. This can be seen in simulation results below where an interferer with slope of $10 \text{ MHz}/\mu\text{s}$ interfered with the ego vehicle which was running at $20 \text{ MHz}/\mu\text{s}$.

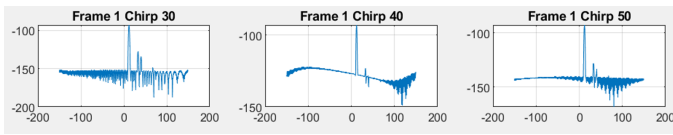


Fig. 5. Noise floor increase due to interference affects all FFT bins, whereas targets appear in positive bins only

If X is an $N_C \times N_{Rx} \times N_S$ input array from a frame. And Y_j is a $1 \times N_{Rx} \times N_S$ array of the RangeFFT on the j^{th} chirp, we define $P(j)$ as:

$$P(j) = \sum_{n=0}^{N_S/2} |Y_j(1, n)|^2$$

if $P(j) > \text{Threshold}$, NDMC is triggered.

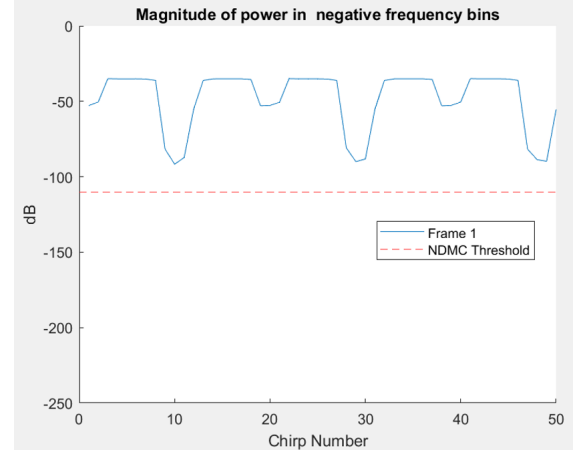


Fig. 6. In this scenario simulation, all chirps in the frame showed power higher than the threshold and NDMC was triggered

- (2) Non-Mutual Data Cancellation (NDMC): Since all interference is most likely to only add to the magnitude of RangeFFT bins, authors in [15] suggest using a min operator across chirps to identify the best sample per bin for RangeFFT. Given that the RADARs under consideration are very likely to be out of sync, seeing at least one good chirp in a frame is a very likely scenario. Further, a way to improve this probability is to introduce time dithering into the system after interference is detected.

If Y is an $N_C \times N_{Rx} \times N_S$ array obtained from the RangeFFT incoming data, sample i of the single chirp RangeFFT R , reconstructed using NDMC is:

$$R(i) = \min_j (Y_j(1, i))$$

here, $i \in [0, N_S], j \in [0, N_C]$.

Further, let us define $\text{Index}(i) = j$ for which $Y_j(1, i)$ is minimum.

- (3) Chirp Health Rating: Based on results from NDMC, we can deduce that whichever chirp contributes the greatest number of samples to the constructed RangeFFT, must be least affected by noise. And processing samples across antennas for that chirp will allow us to extract the best estimate of AoA from an AngleFFT. Using the mode operator, we can say that

$$\text{HealthiestChirp} = \text{mode}(\text{Index})$$

A block diagram of the proposed system is shown in Fig 9:

The negative bins power threshold will vary from receiver to receiver and is mostly dependent on hardware and processing noise. While environmental factors will add to it, the noise floor of the receiver and DSP noise is what is expected to be decisive contributors. And it can hence be calculated and set initially as a part of a calibration routine.

4 IMPLEMENTATION

To evaluate this system, a simulator was built in MATLAB which is described in the block diagram below.

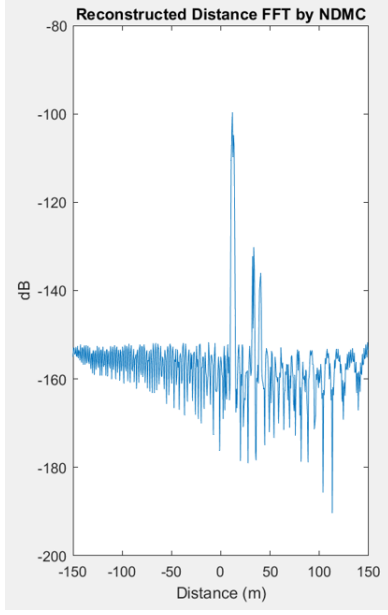


Fig. 7. The reconstructed RangeFFT using NDMC

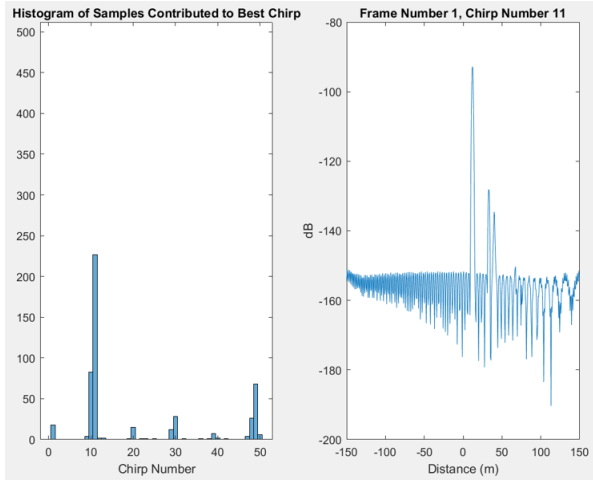


Fig. 8. Histogram of "Index" showing the healthiest chirp and RangeFFT of that chirp

ToF delay was implemented by circular rotation of the transmit chirp waveform. This was done so that effects of time dithering could be clearly emulated. Phase delays at individual antenna elements and doppler delays due to target velocities were implemented by multiplication with appropriate exponentials.

To evaluate and compare performance with and without the mitigation in place, an object finding, and comparison routine were built.

Peaks detected from RangeFFT were filtered to remove those with prominence less than a threshold. Further, locations in the negative bins of RangeFFT were removed. Since most peaks are artefacts of

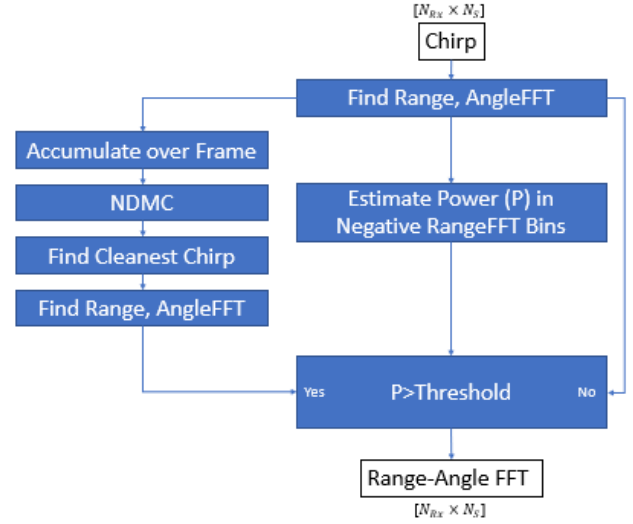


Fig. 9. Proposed SALVAGE Algorithm

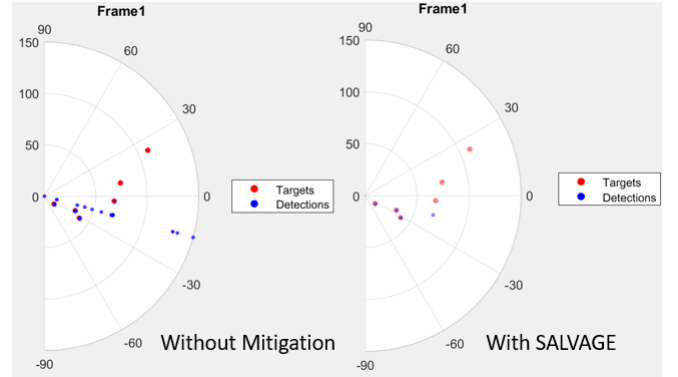


Fig. 10. Comparison of the Point plot generated shows much higher precision when using the SALVAGE algorithm

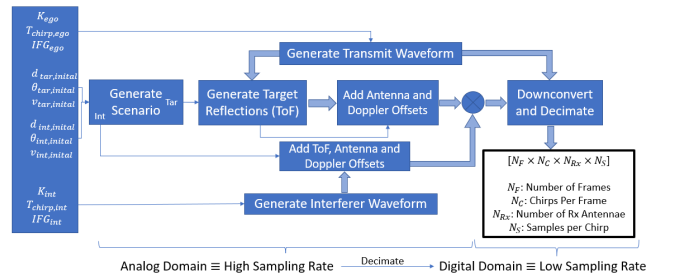


Fig. 11. Block Level Diagram of the MATLAB Simulator used for Validation

sinc sidelobes, the mean of peak magnitudes was used as a rough estimate for Noise floor and peaks below that were removed. Lastly, the first largest peak was chosen as the reference peak and expected magnitudes of peaks at detected locations were calculated based

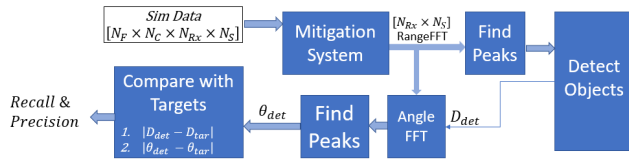


Fig. 12. Block Diagram of the Object Finding and Evaluation Routine

on relative path loss. Any peaks with deviations from this beyond expected RCS variations (± 10 dB, [17]) were eliminated.

AoA was found for the resulting peaks and the set of targets thus detected was compared with those simulated. For comparison of distance from radar, the tolerance was set by the range resolution of $c/(2 * \text{SweepBW})$. Additionally, because ToF was emulated by offsetting samples, more error tolerance was incorporated from the finite sampling frequency in the simulator's "analog domain". For comparison of AoA, the tolerance was set by the angular resolution of $\arcsin(2/(N_{Rx}))$.

5 EVALUATION

For evaluation, the metrics used are defined as follows:

- **Recall:** Also known as True Positive Rate, this is the ratio of targets correctly identified to the total number of targets defined in the scenario. A high recall is desired since it would indicate the ability of our mitigation system to extract target information even in the presence of interferers.
- **Precision:** This is the ratio of targets correctly identified to the total number of targets identified by the system. A high Precision points to the system's ability to pick out only relevant information and eliminate any ghost peaks or spurious peaks.

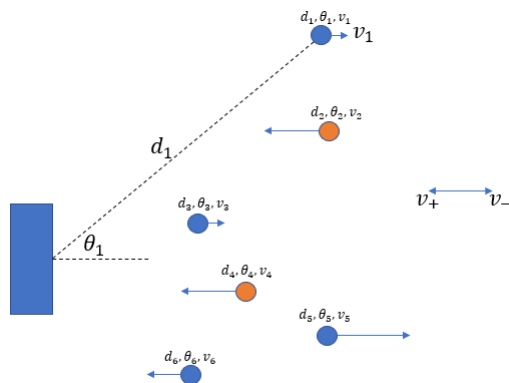


Fig. 13. The conventions used for scenarios simulation

Simulations were carried out with the following parameters:

d_{tar}	v_{tar}	θ_{tar}	d_{int}	v_{int}	θ_{int}	$k_{int}(MHz/\mu s)$
12	-50	-39	18	20	-32	10
33	-20	-25	41	40	-11	17
68	-35	-4	50	50	3	23
75	-65	10	91	90	17	12
110	-70	24	98	100	31	30

- $k_{ego} = 20\text{MHz}/\mu\text{s}$
- $Chirps/Frame_e = 50$
- $ChirpTime = 28\mu\text{s}$
- $NumberOfFrames = 5$

With these parameters, the following scenarios are defined:

- Case 1: No Mitigation
- Case 2: Time Dithering Only
- Case 3: SALVAGE

And following results were obtained for Recall:

Recall (%)				
<i>No.ofInt</i>	<i>Case1</i>	<i>Case2</i>	<i>Case3</i>	
0	100	100	100	
1	17.6	17.4	50	
2	11	11.25	48.57	
3	9.45	9.05	40	
4	6.43	6.67	35.56	
5	6.2	6	32	

Following were the numbers reported for Precision:

Precision (%)			
<i>No.ofInt</i>	<i>Case1</i>	<i>Case2</i>	<i>Case3</i>
0	84.6	83	83
1	34.2	33.11	44.14
2	24.19	24.66	55.5
3	24	23.94	64.5
4	24.22	24.41	66.5
5	23.95	24.14	60

We can see from the above results that:

- SALVAGE provides noticeable improvement in performance even with a basic interpretation engine.
- As the number of interferers increase, we see a decline in performance for all cases. This is expected and SALVAGE still maintains its edge over the No Mitigation or Time Dithering Only cases.
- Time dithering does not show any improvement whatsoever when the interferer has a different slope.
- From the plots, it is also clear that targets farther away suffer most from interference. This is in line with theory which predicts drowning of weak targets due to a rise in noise floor

6 CONCLUSION

We saw how the proposed algorithm can yield up to 40% improvement in the performance of RADAR detection in the presence of interferers. This analysis was limited to Range and AngleFFT. But it can easily be extended to finding doppler by choosing chirps based on their health, albeit with reduced resolution. A better decision

engine based on standards like CFAR would give us a clearer picture to compare with. Because SALVAGE does not actively cancel interference, it suffers from degraded performance as the number of interferers grow and healthy chirps vanish. Clubbing it with an active approach such as filtering might be a useful approach to further improve its performance.

7 REFERENCES

- (1) G. M. Brooker, "Mutual Interference of Millimeter-Wave Radar Systems," in *IEEE Transactions on Electromagnetic Compatibility*, vol. 49, no. 1, pp. 170-181, Feb. 2007, doi: 10.1109/TEM.2006.890223
- (2) M. Goppelt, H.-L. Blöcher, and W. Menzel, "Analytical investigation of mutual interference between automotive FMCW radar sensors," in *German Microwave Conference (GeMIC)*. IEEE, 2011, pp. 1-4
- (3) S. Alland, W. Stark, M. Ali and M. Hegde, "Interference in Automotive Radar Systems: Characteristics, Mitigation Techniques, and Current and Future Research," in *IEEE Signal Processing Magazine*, vol. 36, no. 5, pp. 45-59, Sept. 2019, doi: 10.1109/MSP.2019.2908214.
- (4) M. Kunert, "The EU project MOSARIM: A general overview of project objectives and conducted work," 2012 9th European Radar Conference, Amsterdam, Netherlands, 2012, pp. 1-5.
- (5) Buller, W., Wilson, B., Garbarino, J., Kelly, J., Subotic, N., Thelen, B., & Belzowski, B. (2018, September). Radar congestion study (Report No. DOT HS 812 632). Washington, DC: National Highway Traffic Safety Administration
- (6) Jeong-Geun Kim, Sang-Hoon Sim, Sanghoon Cheon and Songcheol Hong, "24 GHz circularly polarized Doppler radar with a single antenna," 2005 European Microwave Conference, Paris, 2005, pp. 4 pp.-1386, doi: 10.1109/EUMC.2005.1610194.
- (7) Harris et al. (2021). Adaptive filtering for FMCW interference mitigation in PMCW radar systems (U.S. Patent No. 10,976,431 B2). U.S. Patent and Trademark Office.
- (8) Y. Kitsukawa, M. Mitsumoto, H. Mizutani, N. Fukui and C. Miyazaki, "An Interference Suppression Method by Transmission Chirp Waveform with Random Repetition Interval in Fast-Chirp FMCW Radar," 2019 16th European Radar Conference (EuRAD), Paris, France, 2019, pp. 165-168.
- (9) C. Aydogdu, N. Garcia, L. Hammarstrand and H. Wymeersch, "Radar Communications for Combating Mutual Interference of FMCW Radars," 2019 IEEE Radar Conference (RadarConf), Boston, MA, USA, 2019, pp. 1-6, doi: 10.1109/RADAR.2019.8835744.
- (10) L. Hassbring, J. Nilsson. (2020). Machine Learning for FMCW Radar Interference Mitigation [Dissertation], Lund University, Seden, <https://tinyurl.com/4pd295bn>
- (11) M. Barjenbruch, D. Kellner, K. Dietmayer, J. Klappstein and J. Dickmann, "A method for interference cancellation in automotive radar," 2015 IEEE MTT-S International Conference on Microwaves for Intelligent Mobility (ICMIM), Heidelberg, Germany, 2015, pp. 1-4, doi: 10.1109/ICMIM.2015.7117925.
- (12) J. Bechter and C. Waldschmidt, "Automotive radar interference mitigation by reconstruction and cancellation of interference component," 2015 IEEE MTT-S International Conference on Microwaves for Intelligent Mobility (ICMIM), Heidelberg, Germany, 2015, pp. 1-4, doi: 10.1109/ICMIM.2015.7117954.
- (13) F. Jin and S. Cao, "Automotive Radar Interference Mitigation Using Adaptive Noise Canceller," in *IEEE Transactions on Vehicular Technology*, vol. 68, no. 4, pp. 3747-3754, April 2019, doi: 10.1109/TVT.2019.2901493
- (14) M. Barjenbruch, D. Kellner, K. Dietmayer, J. Klappstein and J. Dickmann, "A method for interference cancellation in automotive radar," 2015 IEEE MTT-S International Conference on Microwaves for Intelligent Mobility (ICMIM), Heidelberg, Germany, 2015, pp. 1-4, doi: 10.1109/ICMIM.2015.7117925.
- (15) M. Wagner, F. Sulejmani, A. Melzer, P. Meissner and M. Huemer, "Threshold-Free Interference Cancellation Method for Automotive FMCW Radar Systems," 2018 IEEE International Symposium on Circuits and Systems (ISCAS), Florence, Italy, 2018, pp. 1-4, doi: 10.1109/ISCAS.2018.8351077.
- (16) S. Murali, K. Subburaj, B. Ginsburg and K. Ramasubramanian, "Interference detection in FMCW radar using a complex baseband oversampled receiver," 2018 IEEE Radar Conference (RadarConf18), Oklahoma City, OK, USA, 2018, pp. 1567-1572, doi: 10.1109/RADAR.2018.8378800.
- (17) E. Bel Kamel, A. Peden and P. Pajusco, "RCS modeling and measurements for automotive radar applications in the W band," 2017 11th European Conference on Antennas and Propagation (EUCAP), Paris, France, 2017, pp. 2445-2449, doi: 10.23919/EuCAP.2017.7928266

Received 24 March 2023